Predicting Pacific Decadal Variability

Richard Seager, Alicia R. Karspeck, Mark A. Cane, Yochanan Kushnir

Lamont-Doherty Earth Observatory of Columbia University

Alessandra Giannini

International Research Institute for Climate Prediction

Alexey Kaplan, Ben Kerman, and Jennifer Velez

Lamont-Doherty Earth Observatory of Columbia University

The case is advanced that decadal variability of climate in the Pacific sector is driven by tropical atmosphere-ocean interactions and communicated to the extratropics. It is shown that tropical decadal variations in the last century *could* arise as a consequence of the regional subset of physics contained within an intermediate model of the El Niño-Southern Oscillation. These decadal changes in ENSO and tropical mean climate are more predictable than chance years in advance but even in these idealized experiments forecast skill is probably too small to be useful. Nonetheless, forecasts of the next two decades indicate that, according to this model, the 1998 El Niño marked the end of the post 1976 tropical Pacific warm period.

Observations and atmosphere general circulation models are interpreted to suggest that decadal variations of the atmosphere circulation over the North Pacific between the 1960s and the 1980s are explained by a mix of tropical forcing and internal atmospheric variability. This places a limit on their predictability. The ocean response to extratropical atmosphere variability consists of a local response that is instantaneous and a delayed response of the subtropical and subpolar gyres that is predictable a few years in advance.

It is shown that the wintertime internal variability of the Aleutian Low can weakly impact the ENSO system but its impact on decadal predictability is barely discernible.

1. INTRODUCTION

For four years prior to fall 2002 the mid-latitudes of both the Northern and Southern Hemisphere experienced substantially less rain than usual. In the United States and across Southern Europe into Central Asia wells ran dry, crops failed and forests caught fire. The causes of this dry period have been linked to variations of the tropical atmosphere-ocean system in the Indo-Pacific region [*Hoerling and Kumar,* 2003]. After the enormous El Niño of winter 1997/98 the equatorial Pacific remained cooler than usual until early 2002 when a weak El Niño developed. It could be that this cold period marks the end of the most celebrated decadal variation in the Pacific sector: the warm shift in 1976 [*Zhang et al.,* 1997].

After 1976 the tropical Pacific Ocean has been warmer than in the preceding decades while the central and western North Pacific Ocean have been colder and atmospheric pressure has been lower over the mid-latitude North and South

Earth's Climate: The Ocean-Atmosphere Interaction
Geophysical Monograph Series 147

10.1029/147GM06

Pacific Oceans. In the early 1940s the climate of the Pacific went through a shift in the opposite direction. These characteristics of Pacific Decadal Variability (PDV) have been described by, among others, Graham [1994], Trenberth and Hurrell [1994], Zhang et al. [1997], Mantua et al. [1997] and Garreaud and Battisti [1999].

Decadal variations of the Pacific climate have important consequences for climate over land analogous, but not identical, to the impacts of the El Niño-Southern Oscillation (ENSO) on interannual timescales. For example Mantua et al. [1997] show that when the tropical Pacific is warm (e.g., after 1976) winters are warm across most of North America but cold in the southeastern United States. Winters are dry across mid-latitude North America but are wet in the southwestern United States and Mexico. The persistent anomalies in atmosphere and ocean exert an impact on energy usage, power generation, agriculture, water resources, North Pacific fish stocks and marine ecosystems [*Mantua et al.,* 1997; *Miller and Schneider,* 2000]. Decadal variations of ENSO have also been associated with decadal variations in Australian climate [*Power et al.,* 1999] and the strength of the Indian monsoon [*Krishnamurthy and Goswami,* 2000; *Kumar et al.,* 1999]. Predictions of the state of the Pacific climate on timescales of years to a decade or more could have significant human benefits.

Most work has been motivated by the idea that the adjustment time for the tropical Pacific Ocean is on the order of years and explains interannual variability and that, analogously, PDV must be associated with a different, decadal timescale, ocean process. This led to explanations that PDV originated in the mid-latitude ocean-atmosphere system [*Latif and Barnett,* 1994, 1996]. It was then postulated that changes in the mid-latitude ocean were communicated through the ocean to the tropics, introducing a delay of several years and coupling together mid-latitude and tropical variability [*Gu and Philander*, 1997]. This has been shown, quite conclusively, not to work because the subsurface temperature signal becomes too weak [*Schneider et al.,* 1999]. In contrast, it has been shown that decadal variations of the tropical Pacific Ocean can be accounted for by tropical and subtropical wind forcing alone [*Schneider et al.,* 1999; *Karspeck and Cane,* 2002; *McPhaden and Zhang*, 2002; *Nonaka et al.*, 2002; *Schott et al.* this volume]. Many proposed mechanisms are reviewed in this volume by Wang and Picaut.

To go with the idea that PDV can originate in the tropics, there is ample evidence that extratropical climate variability in the Pacific can be explained in terms of tropical forcing. Trenberth and Hurrell [1994] made this case on the basis of observational analysis while Alexander et al. [2002] used coupled climate models to demonstrate that much of the North Pacific SST variability on both interannual and decadal timescales can be explained as a remote response to tropical forcing.

Here we will continue the argument that PDV originates in the tropics. Section 2 will examine whether decadal changes of the tropical Pacific atmosphere and ocean are predictable. Section 3 will examine whether the extratropical atmospheric response to decadal variations of tropical SST can be simulated. Section 4 will examine whether the response of the extratropical oceans to wind stress variations forced from the tropics can be predicted some years in advance.

This leaves one interesting stone unturned. Pierce et al. [2000], Vimont et al. [2001] and Vimont et al. [2003b] have argued that variability of the North Pacific atmosphere circulation can cause trade wind variability that changes subtropical SSTs and impacts ENSO. Consequently, in Section 5, we will examine the impact on coupled tropical Pacific climate variability of that part of trade wind variability that is associated with the internal, unforced, variability of the extratropical atmosphere.

2. TROPICALLY GENERATED PACIFIC DECADAL VARIABILITY AND ITS PREDICTABILITY

Until proven otherwise, a valid hypothesis for the origin of PDV is that it originates in the tangle of coupled atmosphere-ocean processes within the tropical Pacific that also give rise to interannual ENSO variability. This could arise in two ways. First, the longer timescale modes may arise deterministically (albeit chaotically) from nonlinear interactions among components of interannual variability or via very low frequency modes in the ocean dynamics [*Jin,* 2001]. Second, the application of noise to a system that can only oscillate on interannual timescales will generate variability on decadal timescales. The second method is by definition not predictable on decadal timescales while the first may be if the slow evolution of the ocean state can be predicted.

2.1. Decadal Variability in the Zebiak-Cane Model

Karspeck et al. [2004] (KSC hereafter) considered the first possibility and examined decadal variations within the Zebiak-Cane (ZC) model and their predictability. The ZC model is a geophysical model of the tropical Pacific Ocean and the atmosphere above that is used for studies of ENSO and ENSO prediction (see *Zebiak and Cane* [1987], *Cane et al.* [1986] for a complete model description).

KSC demonstrated that the model is capable of creating realistic decadal variability by searching 150,000 years of simulated unforced natural variability for periods that matched observations. Figure 1 (top) shows one of dozens of 30 year model segments that resemble the observed NINO3 record

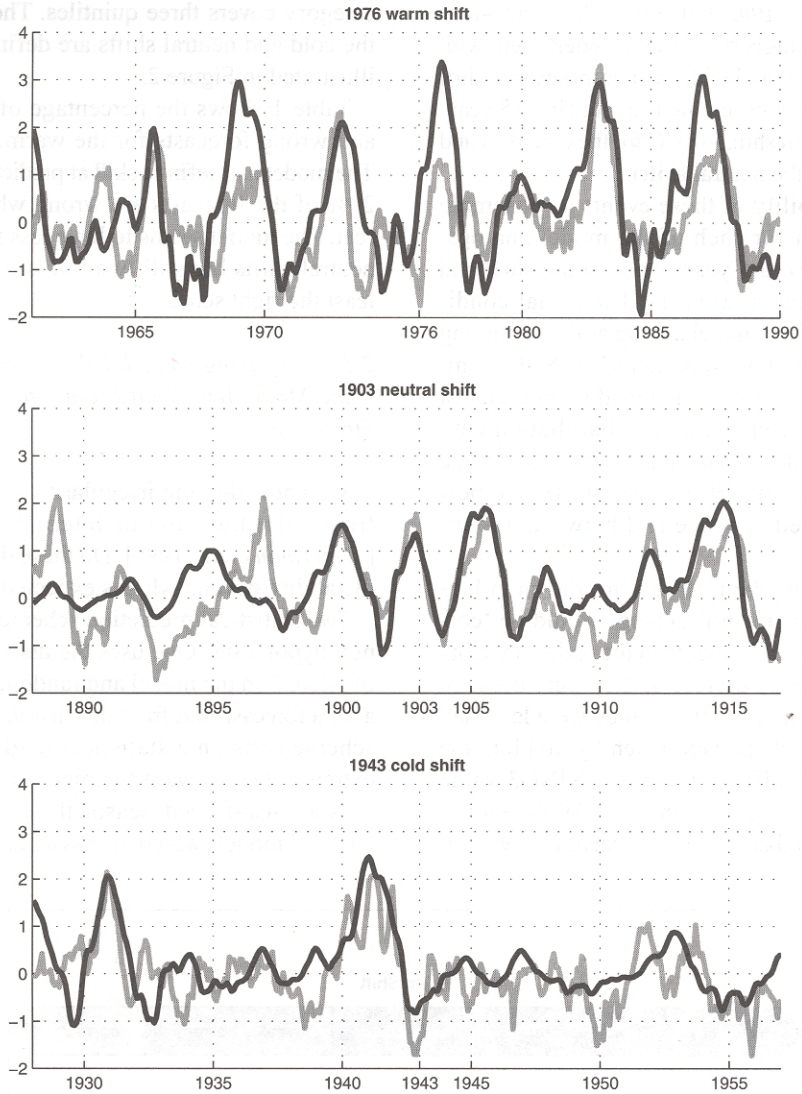

Figure 1. Time series of NINO3 from observations (gray) and the Zebiak-Cane model (black). The model segments were chosen from the long run to match the observed interannual variability and the decadal shifts. The first has a warm shift across 1976 with the 15 years after being warmer than the 15 years before by 0.38°C (observed) and 0.41°C (model), the third has a cold shift across 1943 of –0.32°C (model) and –0.36°C and, for comparison, the second has no shift at all. Taken from KSC.

(the SST anomaly averaged over 5°S–5°N and 90°W–150°W) for the 1961 to 1991 period containing the 1976 warm shift, the unquestioned star of tropical decadal variability. This example has a correlation coefficient with the observed record of 0.59 (using unfiltered monthly data) and has a post 1976 warming (relative to the 15 years before) of 0.41°C compared to the observed 0.38°C. The other two examples shown have equally high correlation to observations and are the 1942 'cold shift' (–0.36°C shift in the model compared to the observed –0.32°C) and, for comparison, a 'neutral shift' centered on 1903 (neither model nor observations had a noticeable shift). Each of these decadal variations can be mimicked by the model. The lesson is that the regional subset of tropical climate physics contained within the ZC model may be sufficient to generate the decadal variations that have occurred in the last 150 years.

2.2. Predictability of Decadal Variability in the Zebiak-Cane Model

KSC identified twenty-four 30 year segments (hereafter called model analogs) for each of the three observed segments

(i.e., those centered on 1976, 1942 and 1903). The twenty-four chosen were those with the highest correlation coefficient with the observed record (all ≥0.5) and with an appropriate size shift in the average temperature between the last and first 15 years of the record (0.3°C for warm shift, –0.3°C for the cold shift and absolute value ≤0.1°C for the neutral shift).

To assess the predictability of these events an ensemble of 100 forecasts was run for each of the model analogs. Each forecast was initialized 5 years prior to the shift and integrated for the subsequent 20 years. The initial condition was the exact state of the model analog at the beginning of the forecast plus a random perturbation in the SST anomaly field. The SST perturbation at each grid point equals a random number sampled from a uniform distribution with zero mean and a standard deviation equal to that at the same place of the 150,000 year model integration. Hence perturbations are uncorrelated in space and between ensemble members.

The criteria for evaluating the forecasts are shown in Figure 2. A forecast of the warm shift analogs would be 'correct' if the later 15 years were warmer than the earlier 15 years by more than 0.21°C, 'weakly correct' if they were between 0.06°C and 0.2°C warmer and 'wrong' if they were less than 0.06°C warmer. These numbers were taken by dividing the statistical distribution of shifts in the mean NINO3 value between concurrent 15 year segments in the 150,000 year run into quintiles with equal numbers of shifts in each. The 'wrong' category covers three quintiles. The success of forecasts of the cold and neutral shifts are defined analogously and also illustrated in Figure 2.

Table 1 shows the percentage of correct, weakly correct and wrong forecasts for the warm, cold and neutral shifts. The model has definite skill at predicting warm shifts: less than 20% of the forecasts are wrong while almost 60% are correct. The model seems to have less skill at predicting cold or neutral shifts but still two thirds of the forecasts shift in at least the right sense.

2.3. Comparing Decadal Predictability in the Zebiak-Cane Model With That From Statistical Forecasting Strategies

We know that the irregularity in the ZC model arises not from noise but from its internal, deterministic dynamics [*Tziperman et al.,* 1995]. Do these dynamics provide any predictability beyond what is expected by chance?

Two statistical prediction schemes were used as strawman null hypotheses. One uses the distribution of 20 year means of NINO3 in the model and randomly grabs the twenty years after a forecast start from this distribution. Forecast skill in this scheme rests on a statistical tendency to shift away from extreme states toward the model mean. The second scheme uses a noise-forced, seasonal, second order autoregressive [AR(2)] model (which allows an oscillation) fitted to the ZC

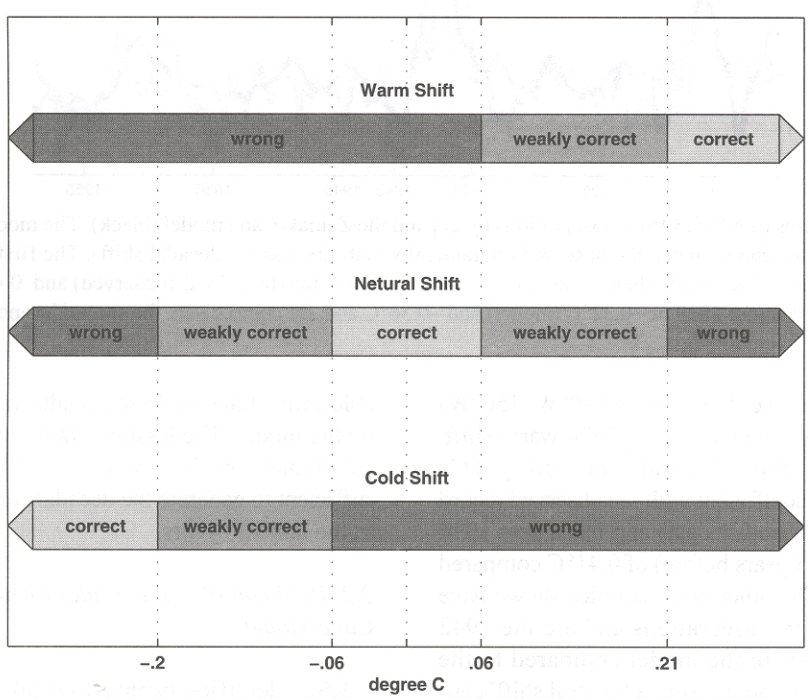

Figure 2. Schematic showing how forecasts are divided into 'correct', 'weakly correct' and 'wrong'.

Table 1. Performance of the dynamical model and two naive forecasting strategies presented as a function of the sense of the shift (warm, neutral or cold). Results for the dynamical model are based on 100 member ensembles for each of the 72 analog series (24 each of warm, neutral and cold shifts). Ensembles of size 500,000 were used for the naive forecasts. Taken from KSC.

	ZC Dynamical Forecasts			Naive Reference Forecasts					
				ZC-Long distribution			AR(2)		
	correct	weak	wrong	correct	weak	wrong	correct	weak	wrong
warm shift	59%	23%	18%	42%	26%	32%	47%	16%	37%
neutral shift	21%	45%	34%	18%	39%	43%	14%	30%	56%
cold shift	41%	23%	36%	30%	22%	48%	34%	14%	52%

model. The first ten years were identical to the model analogs and ensemble forecasts were then performed using different sequences of noise forcing for the 20 years after the forecast initialization.

As shown in Table 1 the ZC model outperforms the two statistical forecasting schemes for all shifts by a modest amount. To assess by how much the ZC model skill exceeds what would be expected by chance we used the Ranked Probability Score (RPS, *Wilks* [1995]), which accounts for how far the forecast is from what actually happened. For each forecast system we compute the fraction correct (f_c), weakly correct (f_{wc}) and wrong (f_w) with $f_c + f_{wc} + f_w = 1$. Then the RPS is given by:

$$RPS = (f_c - 1)^2 + (f_c + f_{wc} - 1)^2.$$

If the forecasts are all correct then RPS = 0 and if they are all wrong then RPS = 2. In between the RPS will get less (i.e. the forecast is better) even when f_c remains the same if f_{wc} increases, thus measuring that the forecasts became closer to the observed state.

The statistical distributions of the RPSs from 5000 100-member ensemble forecasts with each statistical schemes for the warm shift, cold shift and neutral shift are shown in Figure 3. The ZC model forecasts are more skillful than could be accounted for by chance, albeit by a modest amount. The excess predictability of the ZC model must arise from deterministic large scale and coherent evolution of the coupled system.

Instead the statistical model predictive skill, when it arises, comes from knowing at forecast initialization time that conditions have been unusual and that the subsequent 20 years are, statistically speaking, likely to be more akin to climatology (KSC). With only 150 years of observed ENSO variations it is impossible to know the true statistical distribution of decadal shifts and a statistical model based on only that data would probably be a poor tool for decadal prediction, notably worse than the ZC model.

2.4. Forecasting the Future

Extending the work of KSC, we performed a 1000 member ensemble of 30-year ZC model forecasts initialized in December 2002 using the operational data assimilation method outlined in *Chen et al.* [2000]. The initial state of each ensemble member differed by the addition of a random (uncorrelated in space) perturbation of the SST and the sea level height fields with standard deviation of 3°C and 3 cm respectively. Of most interest was the difference in NINO3 for the 15 year period after 1998 minus the 15 year period. Using the same division of shifts into quintiles as before, none of the 1000 forecasts went warm or weakly warm, 2.2% showed no shift, 56.8% went weakly cold and 41% went cold. The model, at least, is convinced that the 1997/8 El Niño marked the end of the post-1976 warm period.

3. PREDICTING DECADAL VARIATIONS OF EXTRATROPICAL ATMOSPHERE CIRCULATION FROM KNOWN SSTS

If decadal variations of tropical Pacific climate are predictable to a modest degree years in advance does this allow prediction of decadal climate variations outside of the tropical Pacific? On interannual timescales the movement of regions of deep convection that occurs within the ENSO cycle forces changes in the tropospheric stationary and transient eddies that create climate anomalies worldwide [*Horel and Wallace,* 1981; *Ropelewski and Halpert,* 1987, 1989; *Sardeshmukh and Hoskins,* 1988; *Held et al.,* 1989; *Hoerling and Ting,* 1994]. It is not so well established that decadal variations of tropical SSTs have an analogous impact.

3.1. Observed Decadal Variations of Atmospheric Circulation

In Figure 4 we show the differences in SST and 500 mb geopotential height during November to March (the season

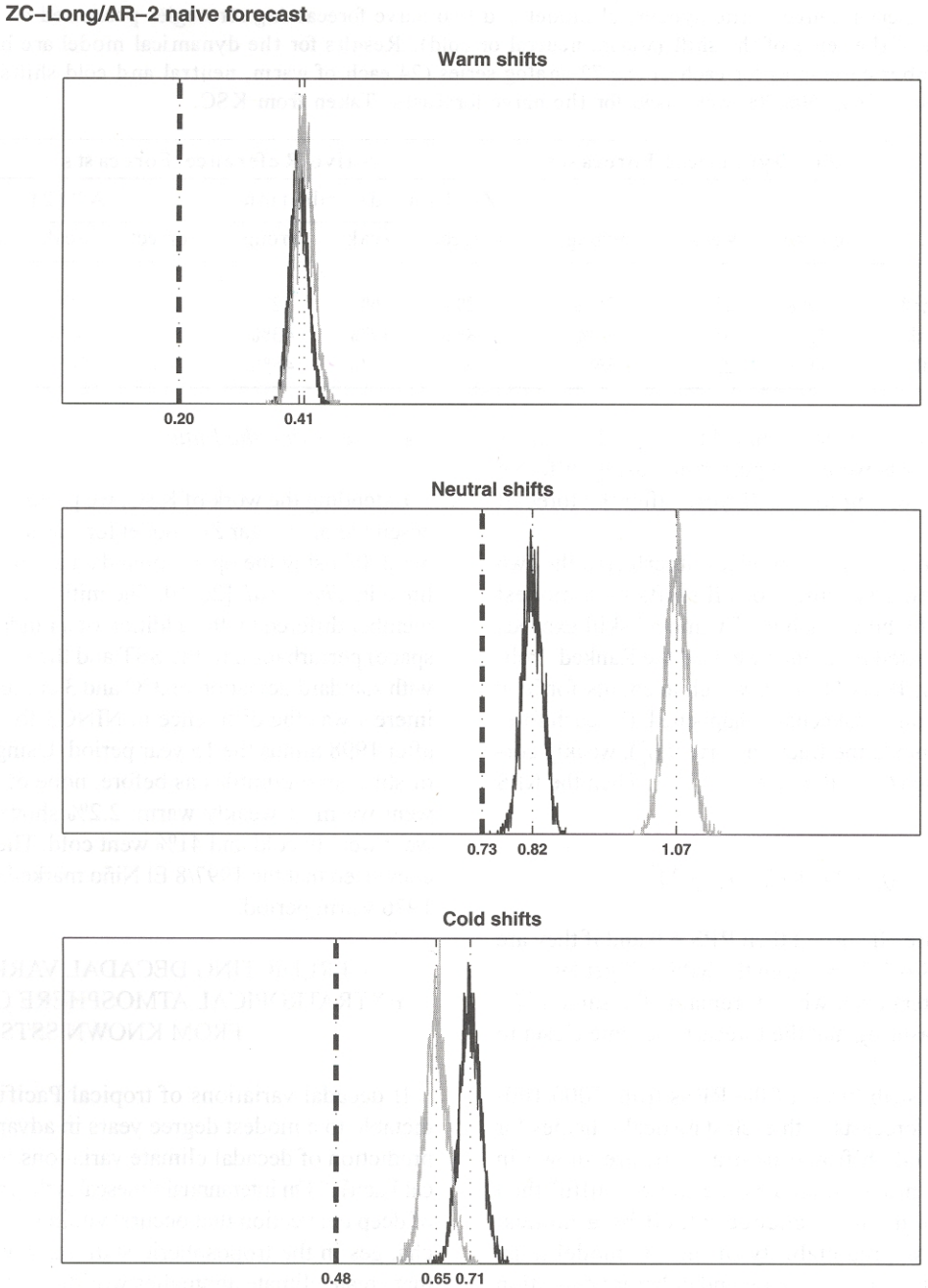

Figure 3. Ranked probability score for the warm shift (top panel), neutral shift (middle panel) and cold shift (bottom panel) forecasts by the ZC model, the AR model (gray) and the naive strategy (black). The RPS scores for the two statistical methods are shown as a distribution of 5000 scores. The ZC scores are shown as a single vertical line. In each case the ZC forecasts are unambiguously more skillful (i.e. RPS closer to 0) than the statistical forecasts. Taken from KSC.

when ENSO-related SST anomalies peak and the one in which the influence of the tropics on the Northern Hemisphere extratropical atmosphere circulation is most marked) for the decade 1977/1978 to 1986/1987 minus the decade 1966/1967 to 1975/1976.

After 1977 the Aleutian Low was anomalously deep (and slightly further south). This was a typical equivalent barotropic signal as evidenced by anomalously low sea level pressure (SLP) below and shifted to the east (not shown). There was anomalous high geopotential height over North America cen-

tered in the northwest. Associated with this circulation shift there was cold water stretching from the coast of Japan to the central North Pacific while the tropics were warm, especially in the east.

This pattern of decadal variability of atmosphere circulation could arise from either internal variability or boundary forcing by variations in SST. A useful first step is to compare the decadal variations with the interannual ones. Figure 5 shows the 500 mb height anomaly for the November through March season regressed onto the NINO3 index, using data from the NCEP-NCAR Reanalysis for 1959 to 1999 thus providing an estimate of the ENSO-forced 500mb variability. It is quite similar to the pattern of decadal variability. Both have low geopotential over the North Pacific (although the decadal low is 20° west of the interannual low) and both have high geopotential over North America and in the tropics. The proportionality between the tropical and mid-latitude height anomalies is similar for both patterns which is strong circumstantial evidence for tropical forcing of each.

3.2. Causes of Decadal Variations of the Atmospheric Circulation

To further examine whether the observed decadal variations of the extratropical atmosphere are caused by internal variability or are boundary forced we performed an ensemble

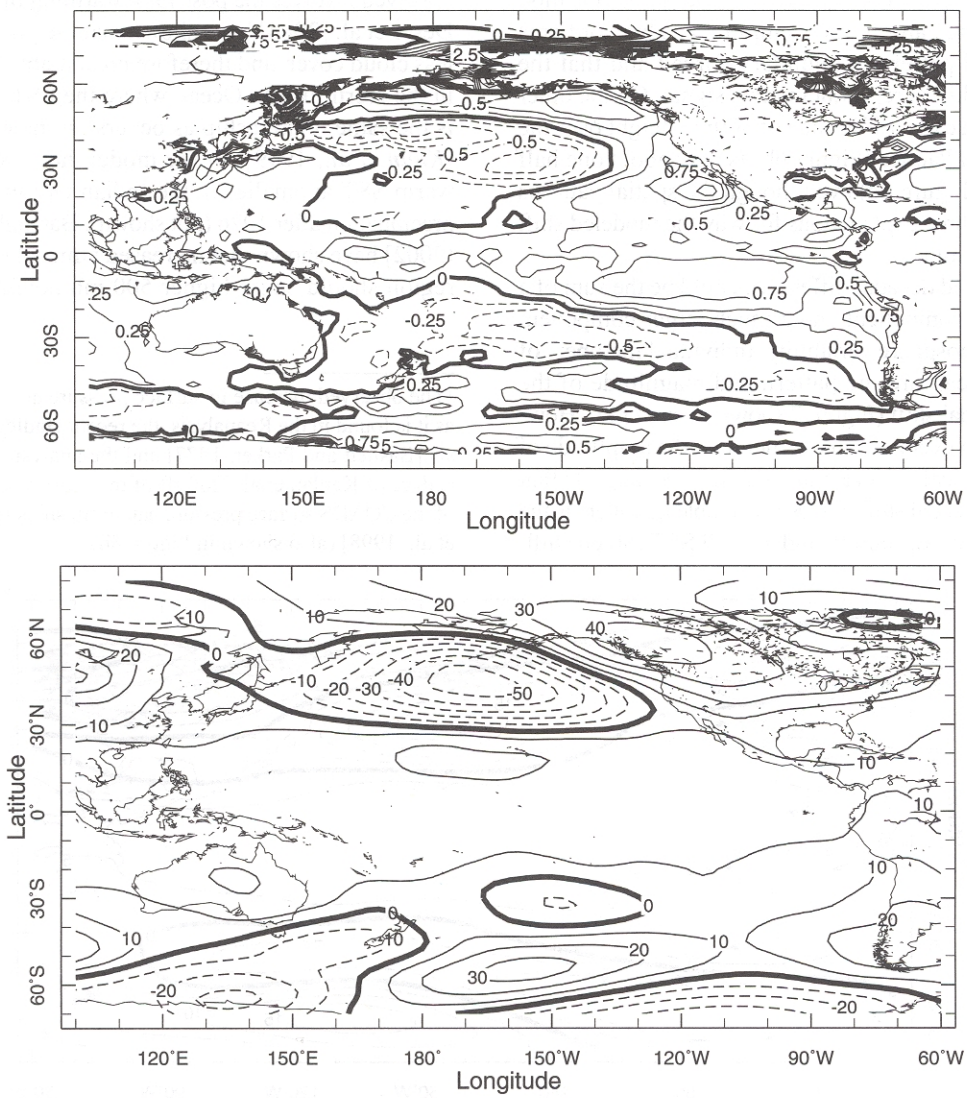

Figure 4. The difference in SST (top panel, contours in Kelvin) and 500mb height (lower panel, contours in meters) for the November to March season for the average of winters from 1977/78 to 1986/87 minus the average of winters from 1966/67 to 1975/76. The data are from the NCEP Reanalysis.

of 16 simulations with the National Center for Atmospheric Research Community Climate Model version 3 (NCAR CCM3, *Kiehl et al.* [1998]). Each ensemble member had different initial conditions but each used the same history of observed SSTs as a lower boundary condition from 1959 to 2000 [*Rayner et al.,* 2003].

For a sufficiently large ensemble, taking the ensemble mean removes the internal variability leaving behind the boundary-forced component. This was confirmed in that two subsequent 16 member ensembles contained temporal and spatial patterns of variability in the ensemble mean that were nearly identical to those shown here. The pattern of modeled interannual variability is shown in Figure 6a and is very similar to that observed (Figure 5) both in terms of the spatial location of principal features and in their amplitude. This confirms that the observed pattern is boundary-forced and that the model has some skill at reproducing this signal. On the other hand, the model decadal difference of 500mb height over the tropical and North Pacific (Figure 6b) is only about one half of that observed (Figure 4b) even though the spatial patterns are very similar. Three explanations for why the modeled shift is weak come to mind.

First, the observed decadal difference could be the sum of a small SST-forced component and a much larger component due to internal atmosphere variability. Individual members of the ensemble do capture the pattern and magnitude of the extratropical decadal shift (Figure 7 shows an example). However, in these, as in every ensemble member, the amplitude of the associated tropical shift remains weak. This suggests that the extratropical decadal shift in these ensemble members is the sum of large internal variability and a small SST-forced shift.

Second, the weak tropical 500mb height shift in the model may itself cause the weak extratropical response along the lines proposed by Seager et al. [2003b]. The weak tropical shift is caused, primarily, by the model's failure to capture the increase in surface to 500mb thickness temperature that occured in 1977 and persisted through 1984 (Figure 8a) and, secondly, by the model's failure to simulate the high surface pressure in the seven years following 1976 (Figure 8b)[1]. Both model failures were reproduced in a similarly-forced 24 member ensemble using the ECHAM4.5 atmosphere model conducted by the International Research Institute for Climate Prediction.

The third possibility for why the decadal shift in the modeled height anomalies over the North Pacific is smaller than observed involves the post 1976 warming of the Indian Ocean. Deser et al. [2004] have shown that the post 1976 period had less cloud cover, and therefore presumably less precipitation, in the North Indian Ocean where the SST was warmer. This is the same relationship as occurs on interannual timescales [*Klein et al.,* 1999]. In the model, however, specifying the warm SST anomalies in the Indian Ocean caused increased precipitation after 1976 (not shown). Barsugli and Sardesmukh [2002] have shown that increased atmospheric heating in this region should cause higher 500 mb heights over the North

[1]The observed increase in surface pressure at this time appears real as it is found in the Reanalysis, the recent Hadley Centre SLP analysis [Basnett and Parker, 1977] and the analysis (following the procedure of Kaplan et al. [2000]) of the most recent release, in 2001, of the COADS surface pressure data from ships and buoys [Woodruff et al., 1998] (also shown in Figure 8b)

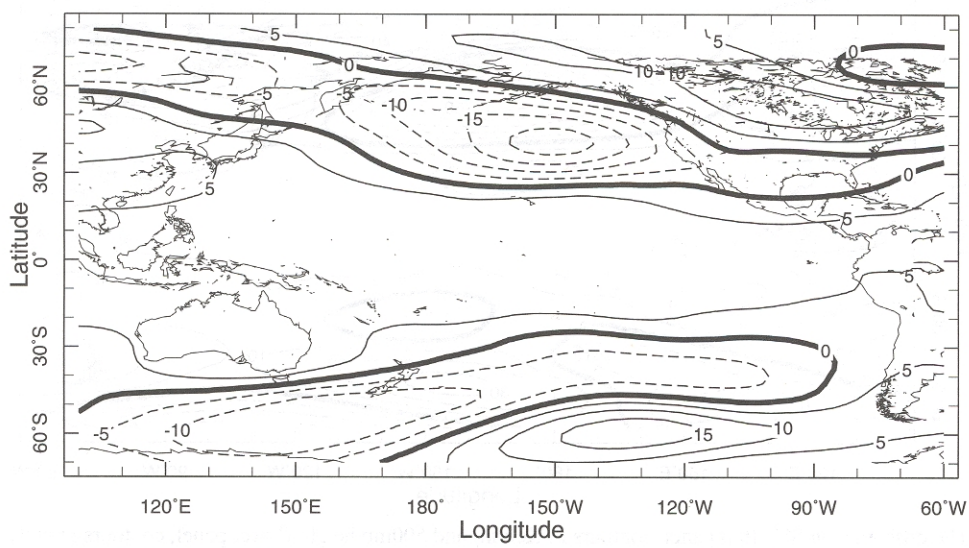

Figure 5. The 500mb height for the November to March season regressed onto the NINO3 index. Contours are meters and the data are from the NCEP Reanalysis.

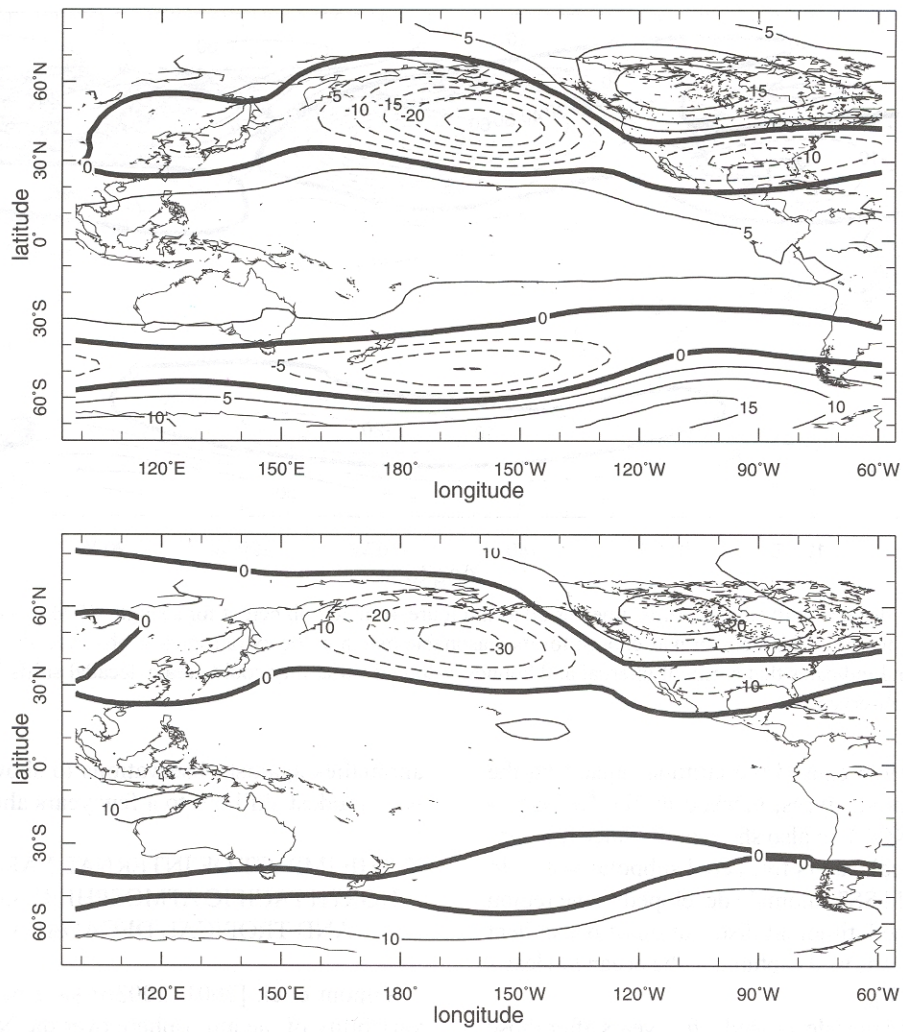

Figure 6. Top panel, same as Figure 5 but for the ensemble mean of 16 integrations of the CCM3 atmosphere model using observed SST in the surface boundary conditions and, lower panel, same as Figure 4b but for the model ensemble mean.

Pacific, opposing the impact of the increased heating over the central tropical Pacific Ocean.

This idea gains some support from a comparison of two 5 member ensembles conducted with CCM3 at the National Center for Atmospheric Research (not shown). One ensemble was forced with observed SSTs everywhere and, akin to our ensemble, had increased precipitation over the Indian Ocean after 1976. The other was forced with observed SSTs in the tropical Pacific Ocean and computed the SST anomalies with a mixed layer ocean elsewhere. This one had no increase in precipitation over the Indian Ocean after 1976 and, consistent with the reasoning above, had a larger drop in 500 mb height over the North Pacific. However, a larger ensemble is needed to prove that imposing Indian Ocean SST anomalies can lead to a mis-estimate of the extratropical response to tropical forcing.

4. PREDICTING THE RESPONSE OF THE NORTH PACIFIC OCEAN TO DECADALLY VARYING WINDS

Tropically-forced wind anomalies over the North Pacific will generate an ocean response. For example, if the tropics force a deeper Aleutian Low, stronger westerlies on the southern side of the Low drive an anomalous southward Ekman flow that cools the SST [*Miller et al.,* 1994; *Seager et al.,* 2001b]. To the east, along the North American coast, southerly wind anomalies warm the SST by warm, moist advection and in the western North Pacific cold, dry advection cools the SST [*Cayan,*1992a, 1992b]. If the anomalous winds over the North Pacific can be predicted so can these local and instantaneous components of the SST response.

Non-local ocean dynamics also come into play [*Seager et al.,* 2001b; *Schneider and Latif,* 2004]. The shift south of the

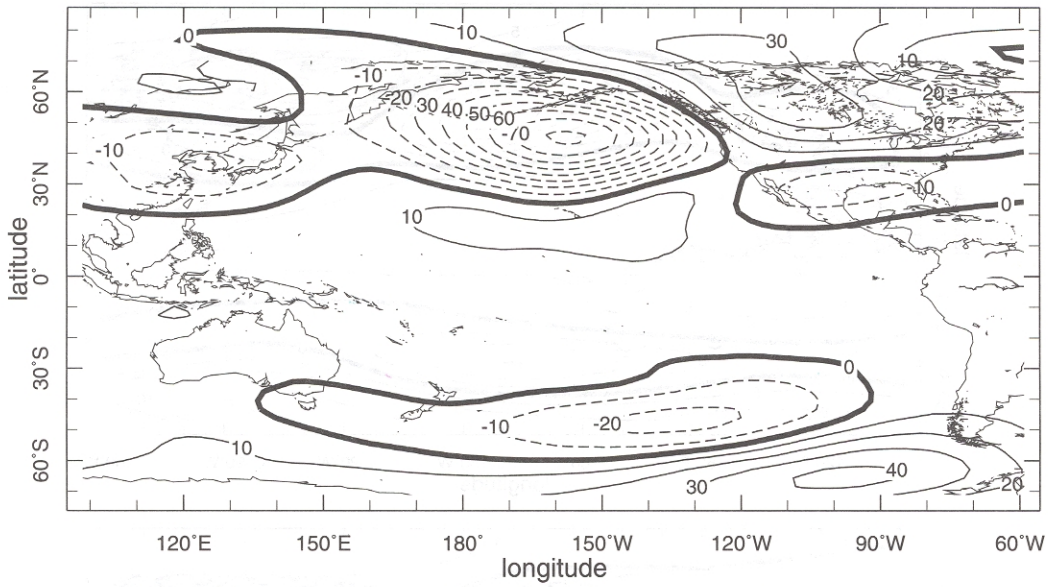

Figure 7. The decadal shift (for the same time period as in Figure 4) in 500mb height for a single CCM3 ensemble member. Units are meters. This member was chosen for its reasonable match in the extratropics to observations in amplitude and pattern and indicates that a mix of internal and boundary-forced variability could create decadal shifts in the extratropics of the observed size.

Aleutian Low after 1976 caused the latitude separating the subtropical and subpolar gyres, marked by the Kuroshio-Oyashio Extension (KOE), to also shift south. Since this separates warm subtropical waters from cool subpolar waters to the north, a potent cold SST anomaly developed in the region it had evacuated as the latitudinal distribution of ocean heat transport altered. This was well captured in the ocean hindcasts of Seager et al. [2001b].

The KOE SST anomalies developed a few years after those in the central Pacific, consistent with the time for westward propagation of oceanic Rossby waves from the region of wind stress forcing. Thus SST variability in the North Pacific involves a response to wind variations that is instantaneous and local in the central Pacific and is delayed and remote in the KOE region (cf. *Nakamura et al.* [1997]).

The delayed response of the gyre circulation has been exploited by Schneider and Miller [2001] to attempt hindcasts of SST anomalies east of Japan. They used a simple time dependent model of thermocline depth in which anomalies at any longitude and time are related to the anomalous wind stress forcing to the east by integrating back in time along Rossby wave characteristics. Hindcasts were performed by integrating the model forward with observed wind stress forcing to the time of the beginning of the hindcast and then continuing with zero wind stress anomaly. As the now unforced Rossby waves continued to propagate west they created thermocline and, by implication, SST anomalies. Schneider and Miller [2001] validated the hindcast SST anomalies against observations to show that the hindcasts have modest skill out to a few years ahead.

5. THE IMPACT OF INTERNAL VARIABILITY OF THE NORTH PACIFIC ATMOSPHERE ON THE TROPICS AND TROPICAL DECADAL VARIABILITY

Vimont et al. [2001, 2003b] have proposed that internal variability of the atmosphere over the North Pacific is associated with variations of the northeast trade wind strength during winter and forces subtropical SST anomalies. They argue that the SST anomalies persist into spring and summer and are damped by anomalous surface fluxes forcing an atmosphere response that includes zonal wind anomalies on the Equator that excite the coupled ocean-atmosphere dynamics familiar in ENSO.

It is difficult to use the observational record to separate between the patterns of internal and boundary-forced variability in the atmosphere. Hence we use the same 16 member SST-forced atmosphere model ensemble as before. Removing the ensemble mean—the boundary-forced component—leaves behind 16 40-year long records of variability generated by internal atmosphere processes alone. We concatenated these records and performed a singular value decomposition (SVD) analysis on the fields of surface wind speed and stress over the subtropical and tropical North Pacific (0°–30°N, to match the tropics-only extent of the ZC model) for the December through February mid winter period. The patterns are shown

in Figure 9 and represent a strengthening and weakening of the northeast trades. These are associated with variations of the Aleutian Low (not shown).

Stronger (weaker) trade winds will tend to cool (warm) the subtropical SSTs via an SST tendency due to increased (decreased) latent heat flux (Q_{LH}) as approximated by $\rho_a C_E L \Delta q U' / \rho_w c_p H$ where ρ_a and ρ_w are the surface air and water densities, Δq is the mean air-sea humidity difference, H is the ocean mixed layer depth, U' is the surface wind speed anomaly and other terms have their usual meaning. To first order wind-forced Q_{LH} variations will be balanced by a compensating change in Q_{LH} due to the SST change (*Seager et al.* [2000b]). In the ZC model that we will use this latter term is represented by $-\alpha T_s'$, where T_s' is the SST anomaly and α is an inverse timescale (*Zebiak and Cane* [1987]).

If U' is varying in mid-winter, T_s' will develop into spring and then decrease as U' goes to zero and the SST anomaly is damped provoking an atmospheric response. First we computed a Q_{LH} anomaly equal to $\rho_a C_E L \Delta q U'$ using U' derived from the SVD analysis (Figure 9) and climatological mean winter values of Δq. We then imposed this flux anomaly as an initial condition in the Zebiak-Cane model and examined the response and the subsequent evolution of the coupled model over the next several months.

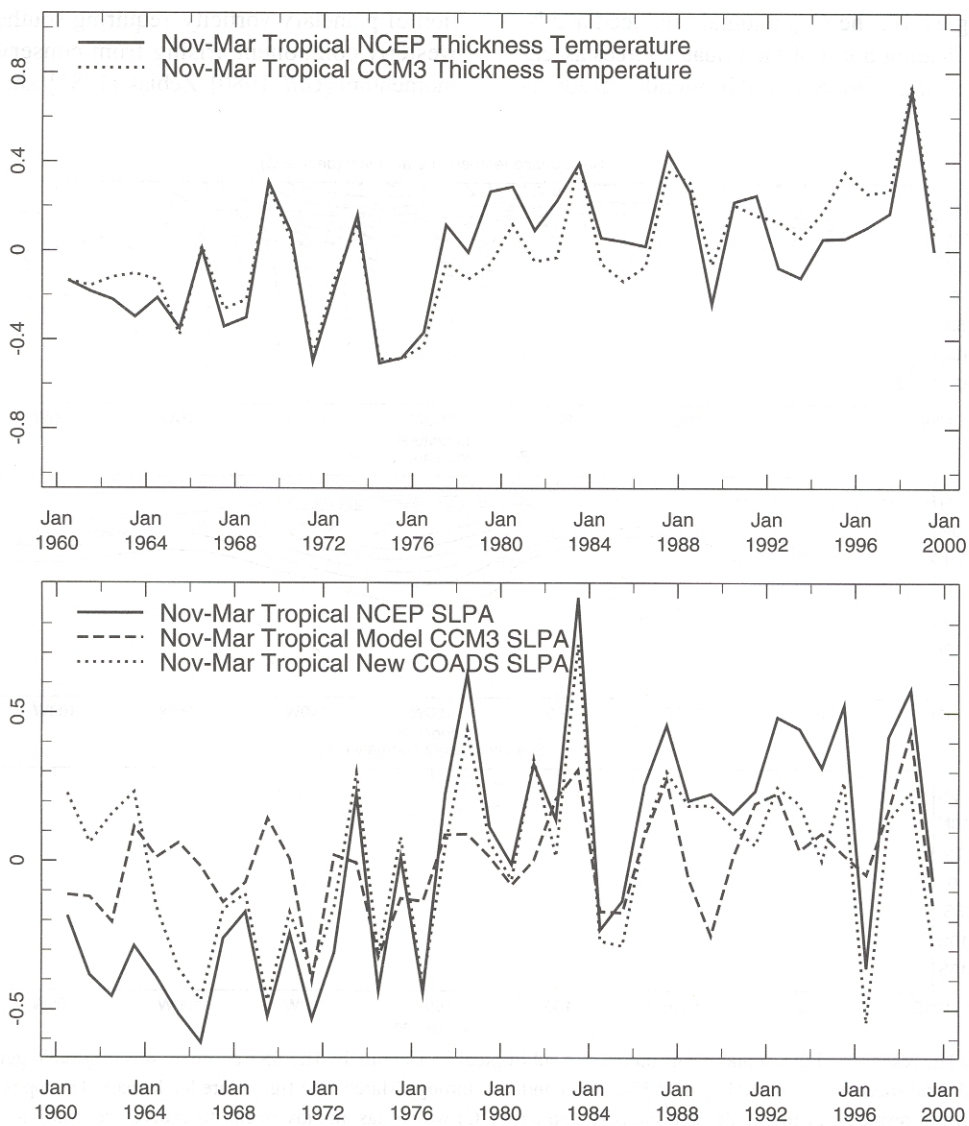

Figure 8. The time history of seasonal means of the tropical mean (20°N to 20°S) anomalies of the thickness temperature (K) between the surface and 500mb from the NCEP Reanalysis and the CCM3 model ensemble mean (top panel) and the SLP (mb) from NCEP Reanalysis, the CCM3 model ensemble mean and a new analysis of COADS ship data (lower panel).

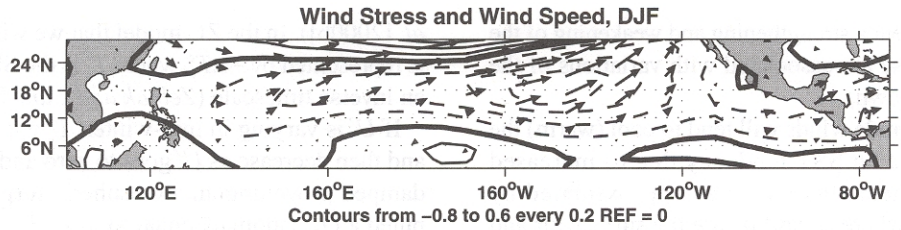

Figure 9. The pattern associated with the first singular vector of an analysis of wind stress (arrows) and wind speed (contours) within an SST-forced ensemble of atmosphere GCM integrations. Before the analysis was performed the ensemble mean, representing the SST anomaly-forced component of variability, was removed. The pattern therefore represents the dominant pattern in the model of internal atmosphere variability over the subtropical North Pacific. It accounts for 28% of the total variance in the fields. The maximum anomalous wind speeds are about $1 ms^{-1}$ and the maximum stress anomalies, corresponding to the longest arrows, are of magnitude about $0.02\ Nm^{-2}$.

As shown in Figure 10, the Q_{LH} anomaly induced a subtropical warming. Heating north of the Equator forces ascent with the vortex stretching being balanced by meridional advection of planetary vorticity, requiring southerly flow, and the westerly component arising from conservation of angular momentum [*Gill,* 1980]. Zebiak [1982] shows that, when the

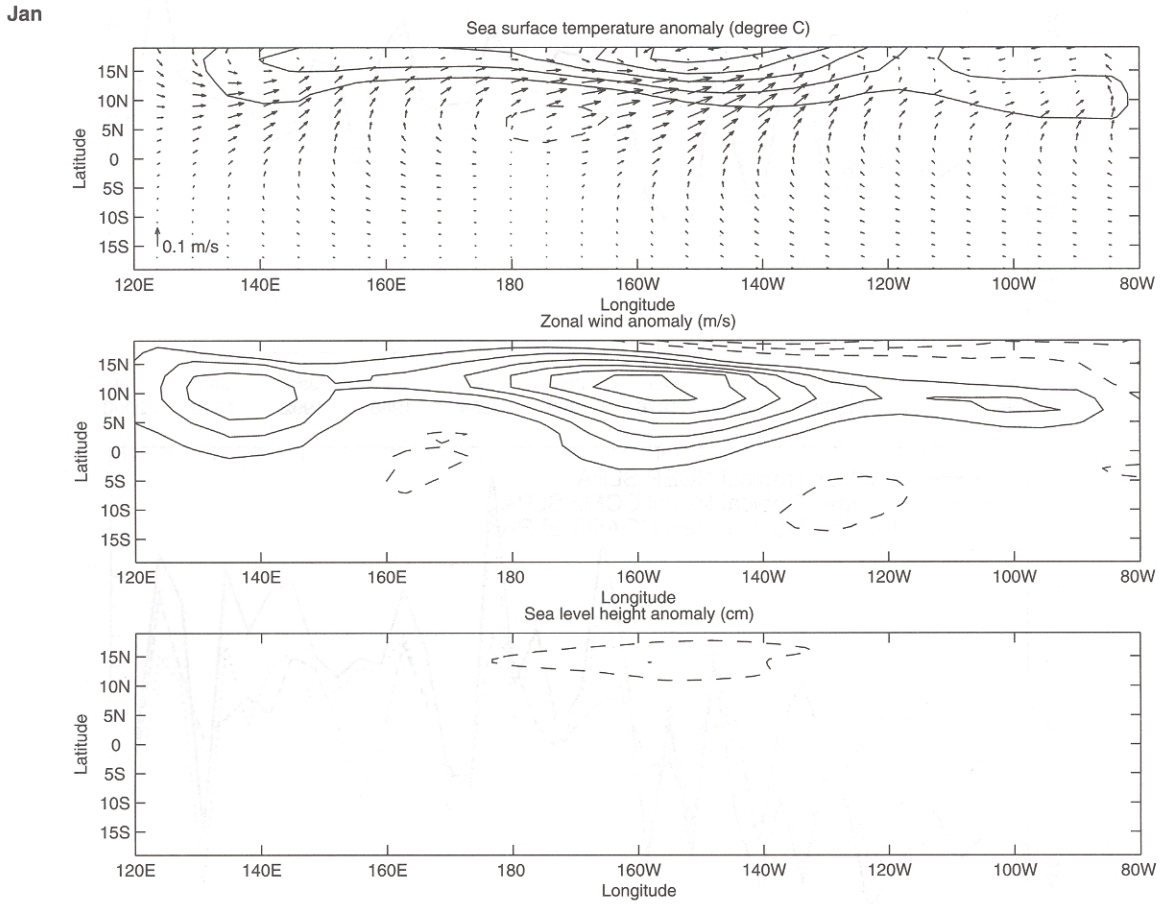

Figure 10. The response of the Zebiak-Cane model to a subtropical SST anomaly. The SST anomaly was originally generated by an imposed wind speed anomaly that begins in November and lasts through March. The figures are for January. The top panel shows the initial wind response of the model and the SST anomaly (°C) which has already begun to evolve according to the model physics. The middle panel shows the associated zonal wind speed response (ms^{-1}) in the model and the lower panel shows the sea level height response (cm). The arrow length of the wind vector is indicated in (a), the contour intervals are 0.03K for the SST anomaly, $0.02 ms^{-1}$ for the zonal wind speed anomaly, 0.3cm for the sea level height anomaly and the zero contours are supressed.

heating north of the Equator is localized in longitude, the southwesterly anomaly extends onto the Equator. The initial ocean response has higher sea level height (SLH), or deeper thermocline, in the central Pacific. As the ocean response evolves (Figure 11), the equatorial southwesterlies force a downwelling oceanic Kelvin wave that propagates east raising SLH and depressing the thermocline in the eastern equatorial Pacific. This immediately causes SST warming in the east and a few months later a classic El Niño pattern develops (Figure 12), albeit with small amplitude, ~0.3°C. Is this impact potent enough to influence ENSO evolution and decadal predictability?

To examine this we add a Q_{LH} anomaly proportional to U' to the SST equation of the Zebiak-Cane model:

$$\frac{\partial T'_s}{\partial t} + dynamics = -\alpha T'_s + bU'f(t).$$

The term 'dynamics' is standing in for the three dimensional advection processes within the model mixed layer. The coefficient b is, for simplicity, taken to be a constant. The function $f(t)$ accounts for the time dependence of the wind speed forcing. It is zero between April and October and then increases to a maximum absolute value in January before declining. It has the same sign throughout each winter season to represent low frequency variability of the trade winds but its value varies randomly from year to year according to a white noise process. Forcing is only imposed in the Northern Hemisphere.

A long run of the ZC model with the subtropical wind forcing imposed was generated and searched for analogs of the observed decadal variability. Hindcasts of these were conducted as before except that, rather than imposing SST perturbations at the start of the forecast, each forecast was continued with a different sequence of subtropical wind speed forcing. Forecast skill was assessed as before and is shown in Table 2 along with the performance of the two statistical forecasting strategies, both of which were regenerated using the data from the long, subtropical forced, model run.

The percentage in each forecast category is very similar to that in the forecasts without noise forcing (Table 1) and the ZC model skill remains modestly higher than that of the statistical schemes. These experiments demonstrate that the skill of the ZC

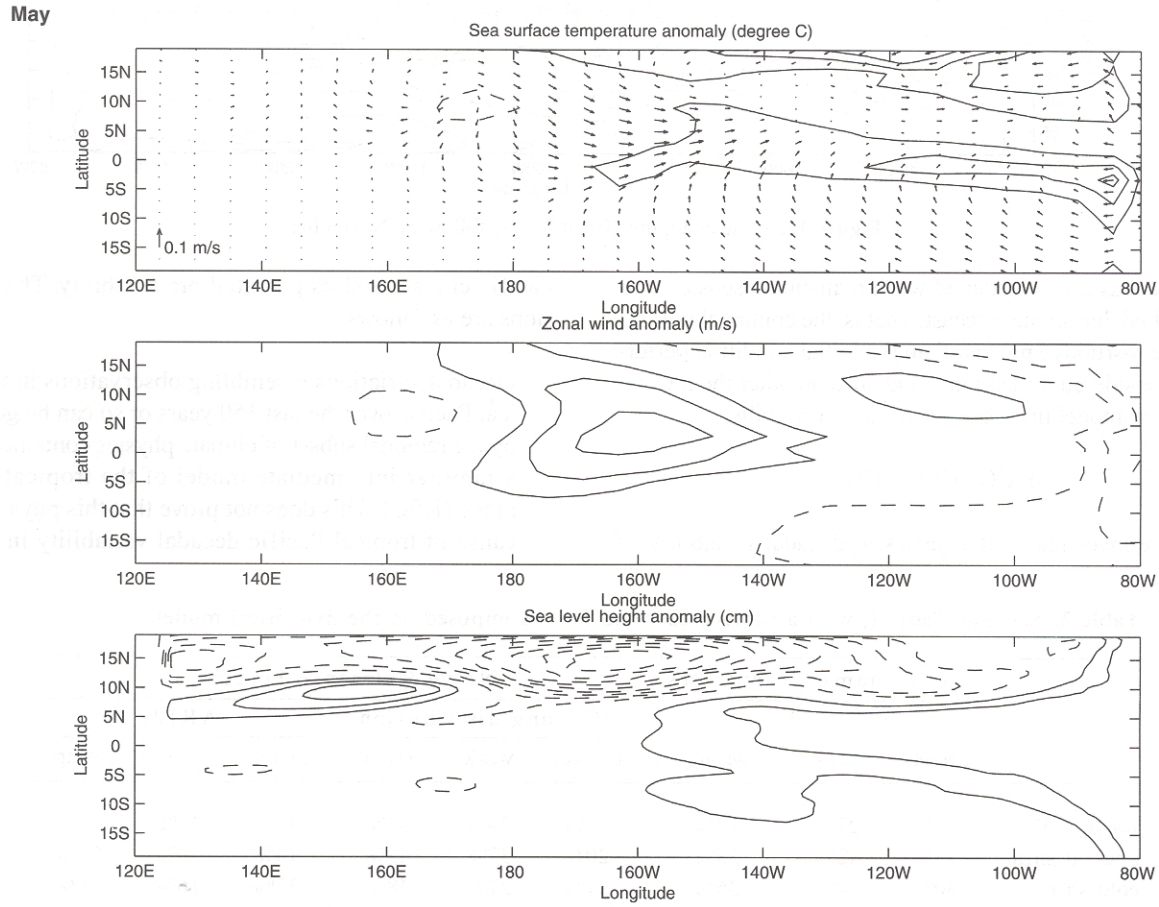

Figure 11. Same as Figure 10 but for the following May.

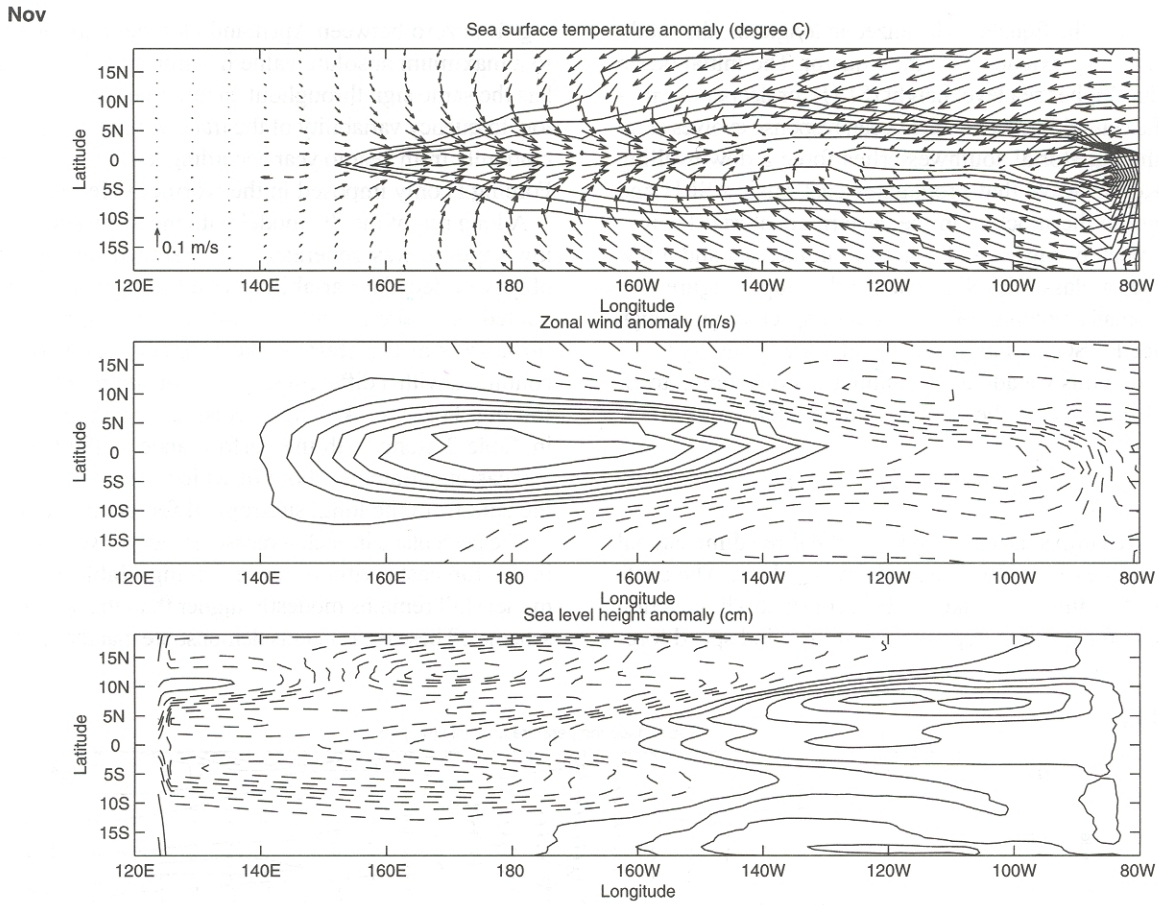

Figure 12. Same as Figure 10 but for the following November

model, such as it is, is retained when realistic noise is continually applied during the forecast. That is, the continual noise is a no more disruptive process than the initial condition perturbations considered in Section 2 and does not alter the mechanisms in the model that generate decadal variability.

6. CONCLUSIONS

We have investigated the causes of decadal variability of Pacific climate and its potential predictability. The conclusions are as follows:

- Decadal variations resembling observations in the tropical Pacific over the last 150 years or so can be generated by the regional subset of climate physics contained within a familiar intermediate model of the tropical Pacific alone (KSC). This does not prove that this physics is the cause of tropical Pacific decadal variability in the real

Table 2. Same as Table 1, with a subtropical wind forcing imposed on the dynamical model.

	ZC Dynamical Forecasts			Naive Reference Forecasts					
				ZC-Long distribution			AR(2)		
	correct	weak	wrong	correct	weak	wrong	correct	weak	wrong
warm shift	54%	27%	19%	43%	24%	33%	48%	17%	35%
neutral shift	23%	42%	35%	20%	37%	43%	14%	30%	56%
cold shift	40%	24%	36%	31%	21%	48%	33%	16%	51%

world but it does make a case that it is not immediately necessary to invoke processes in other regions of the world.

- The model analogs of observed decadal variations, such as the 1976 warm shift, are predictable years in advance. The skill of the geophysical model significantly exceeds that of statistical schemes but is too modest to hold out much hope for useful decadal forecasts (KSC). For what it is worth the model predicts that the 1998 El Niño ended the post-1976 tropical Pacific warm period.

- Decadal variations of tropical Pacific climate drive decadal variations of extratropical climate that could be predicted if the changes in tropical SST were known. Unpredictable internal atmospheric processes can cause equivalent size decadal variations of extratropical climate over the North Pacific. Furthermore, atmosphere models forced by observed SSTs everywhere poorly simulate the tropical response to decadal variations of SST.

- Part of the response of the extratropical North Pacific ocean to decadal variations of the winds involves a delayed adjustment of the subtropical and subpolar gyres. This component causes SST anomalies in the Kuroshio-Oyashio Extension region and is predictable on the timescale it takes for Rossby waves to propagate west to the Asian coast, that is, years [*Seager et al.,* 2001b; *Schneider and Miller,* 2001].

- Internal wintertime variability of the atmosphere over the North Pacific is capable of generating a coupled dynamical response that is ENSO-like but it is weak and does not significantly perturb the decadal predictability of the ZC model.

In summary, a case can be made that Pacific Decadal Variability arises through coupled interactions in the tropics and is communicated to the extratropics. Aspects of this variability are predictable years in advance but the skill is so low that the prospects for useful operational prediction are poor.

Acknowledgments. This work was supported by National Oceanic and Atmospheric Administration grants UCSIO CU 02165401SCF and NA16GP2024 and by National Science Foundation grant ATM-9986072. We thank David Battisti and Clara Deser for valuable discussions, Dake Chen for guidance in hindcasting and forecasting and Ed Sarachik for first suggesting this work. This is Lamont Doherty Earth Observatory Contribution Number 6578.

REFERENCES

Alexander, M. A., I. Blade, M. Newman, J. R. Lanzante, N.-C. Lau, and J. D. Scott, The atmosphere bridge: The influence of ENSO teleconnections on air-sea interaction over the global ocean, *J. Clim.*, *15*, 2205–2231, 2002.

Barsugli, J. J., and P. D. Sardeshmukh, Global atmospheric sensitivity to tropcial SST anomalies throughout the Indo-Pacific basin, *J. Clim.*, *15*, 3427–3442, 2002.

Basnett, T. A., and D. E. Parker, Development of the global mean sea level pressure data set GMSLP2., *Tech. Rep. 79*, Hadley Center for Climate Research, 1997.

Cane, M. A., S. E. Zebiak, and S. C. Dolan, Experimental forecasts of El Niño, *Nature*, *321*, 827–832, 1986.

Cayan, D., Latent and sensible heat flux anomalies over the northern oceans: The connection to monthly atmospheric circulation, *J. Clim.*, *5*, 354–369, 1992a.

Cayan, D., Latent and sensible heat flux anomalies over the northern oceans: Driving the sea surface temperature, *J. Phys. Oceanogr.*, *22*, 859–881, 1992b.

Chen, D., M. A. Cane, S. E. Zebiak, R. Canizares, and A. Kaplan, Bias correction of an ocean-atmosphere coupled model, *Geophys. Res. Lett.*, *27*, 2585–2588, 2000.

Deser, C., A. S. Phillips, and J. W. Hurrell, Pacific interdecadal climate variability: Linkages between the tropics and the North Pacific during boreal winter since 1900, *J. Clim.*, in press, 2004.

Garreaud, R. D., and D. S. Battisti, Interannual (ENSO) and interdecadal (ENSO-like) variability in the southern hemisphere tropospheric circulation., *J. Clim.*, *12*, 2113–2123, 1999.

Gill, A. E., Some simple solutions for heat induced tropical circulation, *Q. J. R. Meteorol. Soc.*, *106*, 447–462, 1980.

Graham, N., Decadal-scale climate variability in the tropical and North Pacific during the 1970s and 1980s: observations and model results, *Clim. Dyn.*, *10*, 135–162, 1994.

Gu, D., and S. G. H. Philander, Interdecadal climate fluctuations that depend on exchanges between the tropics and extratropics, *Science*, *275*, 805–807, 1997.

Held, I., S. W. Lyons, and S. Nigam, Transients and the extratropical response to El Niño, *J. Atmos. Sci.*, *46*, 163–176, 1989.

Hoerling, M. P., and A. Kumar, The perfect ocean for drought, *Science*, *299*, 691–694, 2003.

Hoerling, M. P., and M. Ting, Organization of extratropical transients during El Niño, *J. Clim.*, *7*, 745–766, 1994.

Horel, J. D., and J. M. Wallace, Planetary scale atmospheric phenomena associated with the Southern Oscillation, *Mon. Weather Rev.*, *109*, 813–829, 1981.

Jin, F.-F., Low-frequency modes of tropical ocean dynamics, *J. Clim.*, *14*, 3874–3881, 2001.

Kaplan, A., Y. Kushnir, and M. A. Cane, Reduced space optimal interpolation of historical marine sea level pressure: 1854-1992, *J. Clim.*, *13*, 2987–3002, 2000.

Karspeck, A., and M. A. Cane, Tropical Pacific 1976/77 climate shift in a linear wind-driven model, *J. Phys. Oceanogr.*, *32*, 2350–2360, 2002.

Karspeck, A., R. Seager, and M. A. Cane, Predictability of tropical Pacific decadal variability in an intermediate model, *J. Clim.*, in press, 2004.

Kiehl, J. T., J. J. Hack, G. B. Bonan, B. A. Bovile, D. L. Williamson, and P. J. Rasch, The National Center for Atmospheric Research Community Climate Model: CCM3, *J. Clim.*, *11*, 1131–1149, 1998.

Klein, S. A., B. J. Soden, and N. Lau, Remote sea surface temperature variations during ENSO: Evidence for a tropical atmospheric bridge, *J. Clim.*, *12*, 917–932, 1999.

KrishnaKumar, K., B. Rajagopolan, and M. A. Cane, On the weakening relationship between the Indian monsoon and ENSO, *Science*, *284*, 2156–2159, 1999.

Krishnamurthy, V., and B. N. Goswami, Indian monsoon-ENSO relationship on interdecadal timescale, *J. Clim.*, *13*, 579–595, 2000.

Latif, M., and T. P. Barnett, Causes of decadal climate variability over the North Pacific/North American sector, *Science*, *266*, 634–637, 1994.

Latif, M., and T. P. Barnett, Decadal climate variability over the North Pacific and North America: Dynamics and predictability, *J. Clim.*, *9*, 2407–2423, 1996.

Mantua, N. J., S. R. Hare, Y. Zhang, J. M. Wallace, and R. C. Francis, A Pacific interdecadal climate oscillation with impacts on salmon production, *Bull. Am. Meteorol. Soc.*, *78*, 1069–1079, 1997.

McPhaden, M. J., and D. Zhang, Slowdown of the meridional overturning circulation in the upper Pacific Ocean, *Nature*, *415*, 603–608, 2002.

Miller, A. J., and N. Schneider, Interdecadal climate regime dynamics in the North Pacific Ocean: Theories, observations and ecosystem impacts, *Prog. Oceanogr.*, *47*, 355–379, 2000.

Miller, A. J., D. R. Cayan, T. P. Barnett, N. E. Graham, and J. M. Oberhuber, Interdecadal variability of the Pacific Ocean: Model response to observed heat flux and wind stress anomalies, *Clim. Dyn.*, *9*, 287–302, 1994.

Nakamura, H., G. Lin, and T. Yamagata, Decadal climate variability in the North Pacific during the recent decades, *Bull. Am. Meteorol. Soc.*, *78*, 2215–2225, 1997.

Nonaka, M., S.-P. Xie, and J. P. McCreary, Decadal variations in the subtropcial cells and equatorial Pacific SST, *Geophys. Res. Lett.*, *29*, doi: 10.1029/2001GL013676, 2002.

Pierce, D. W., T. P. Barnett, and M. Latif, Connections between the Pacific Ocean tropics and midlatitudes on decadal timescales, *J. Clim.*, *13*, 1173–1194, 2000.

Power, S., F. Tseitkin, V. Mehta, B. Lavery, S. Trock, and N. Holbrook, Decadal climate variability in Australia during the twentieth century, *Int. J. Climatol.*, *19*, 169–184, 1999.

Rayner, N., D. Parker, E. Horton, C. Folland, L. Alexander, D. Rowell, E. Kent, and A. Kaplan, Global analyses of sea surface temperature, sea ice, and night marine air temperature since the late nineteenth century, *J. Geophys. Res.*, *108*, doi: 10.1029/2002JD002670, 2003.

Ropelewski, C. F., and M. S. Halpert, Global and regional scale precipitation patterns associated with the El Niño/Southern Oscillation, *Mon. Weather Rev.*, *114*, 2352–2362, 1987.

Ropelewski, C. F., and M. S. Halpert, Precipitation patterns associated with the high index phase of the Southern Oscillation, *J. Clim.*, *2*, 268–284, 1989.

Sardeshmukh, P. D., and B. J. Hoskins, The generation of global rotational flow by steady idealized tropical divergence, *J. Atmos. Sci.*, *45*, 1228–1251, 1988.

Schneider, N., and A. J. Miller, Predicting western North Pacific Ocean climate, *J. Clim.*, *14*, 3997–4002, 2001.

Schneider, N., S. Venzke, A. J. Miller, D. W. Pierce, T. O. Barnett, C. Deser, and M. Latif, Pacific thermocline bridge revisted, *Geophys. Res. Lett.*, *26*, 1329–1332, 1999.

Schott, F. A., J. P. McCreary, and G. C. Johnson, Shallow overturning circulations of the tropical-subtropical oceans, this volume.

Seager, R., Y. Kushnir, M. Visbeck, N. Naik, J. Miller, G. Krahmann, and H. Cullen, Causes of Atlantic Ocean climate variability between 1958 and 1998, *J. Clim.*, *13*, 2845–2862, 2000.

Seager, R., Y. Kushnir, N. Naik, M. A. Cane, and J. Miller, Wind-driven shifts in the latitude of the Kuroshio-Oyashio extension and generation of SST anomalies on decadal timescales, *J. Clim.*, *14*, 4249–4265, 2001.

Seager, R., N. Harnik, Y. Kushnir, W. Robinson, and J. Miller, Mechanisms of hemispherically symmetric climate variability, *J. Clim.*, *16*, 2960–2978, 2003.

Trenberth, K., and J. W. Hurrell, Decadal atmosphere-ocean variations in the Pacific, *Clim. Dyn.*, *9*, 303–319, 1994.

Tziperman, E., M. A. Cane, and S. E. Zebiak, Irregularity and locking to the seasonal cycle in an enso prediction model as explained by the quasi-periodicity route to chaos, *J. Atmos. Sci.*, *52*, 293–306, 1995.

Vimont, D., D. S. Battisti, and A. C. Hirst, Footprinting: a seasonal link between the mid-latitudes and tropics, *Geophys. Res. Letters*, *28*, 3923–3926, 2001.

Vimont, D., J. M. Wallace, and D. S. Battisti, The seasonal footprinting mechanism in the Pacific; implications for ENSO, *J. Clim.*, *16*, 2668–2675, 2003.

Wang, C., and J. Picaut, Understanding ENSO physics—A review, this volume.

Wilks, D. S., *Statistical methods in the atmospheric sciences*, 467 pp, Academic Press, San Diego, 1995.

Woodruff, S., R. Slutz, R. Jenne, and P. Steurer, COADS Release 2: Data and metadata enhancements for improvements of marine surface flux fields, *Phys. Chem. Earth*, *2*, 517–527, 1998.

Zebiak, S. E., A simple atmospheric model of relevance to El Niño, *J. Atmos. Sci.*, *39*, 2017–2027, 1982.

Zebiak, S. E., and M. A. Cane, A model El Niño-Southern Oscillation, *Mon. Weather Rev.*, *115*, 2262–2278, 1987.

Zhang, Y., J. M. Wallace, and D. S. Battisti, ENSO-like decade-to-century scale variability: 1900-93, *J. Clim.*, *10*, 1004–1020, 1997.

A. Giannini, International Research Institute for Climate Prediction, Palisades, New York 10964-8000. (alesall@iri.columbia.edu)

R. Seager, A. R. Karspeck, M. A. Cane, Y. Kushnir, A. Kaplan, B. Kerman and J. Velez, Lamont-Doherty Earth Observatory of Columbia University, Palisades, New York 10964-8000. (rich@maatkare.ldeo.columbia.edu)